

## 3D STRUCTURAL REGIONAL MODEL OF THE EGS SOULTZ SITE (NORTHERN UPPER RHINE GRABEN, FRANCE): INSIGHTS AND PERSPECTIVES

P. Baillieux<sup>1</sup>, E. Schill<sup>1</sup>, C. Dezayes<sup>2</sup>

<sup>1</sup>Centre of Hydrogeology and Geothermics (CHYN),  
Neuchâtel University, Rue Emile Argand 11,  
CH-2000, Neuchâtel, Switzerland

<sup>2</sup>BRGM (French Geological Survey)  
3, avenue Claude Guillemin,  
BP36009, F-45060, Orléans Cedex 2, France

e-mail: paul.baillieux@unine.ch

### **ABSTRACT**

In a perspective of geothermal exploration in graben systems, we analyse the recently built consistent structural model of Soultz area (Dezayes *et al.*, this issue) in order to understand the links between the regional graben fault system, the tectonic history of the Upper Rhine Graben (URG) and the local reservoir features (a low permeable naturally fractured granite).

The previous geological models of the area lack constraints concerning the geometry of the structures at the regional scale. To overcome this situation, the new 3D regional geological model of the Soultz area is based on a set of 2D seismic profiles (including recently reprocessed seismic lines) as well as former structural interpretations for oil exploration in the 70-80's and numerous deep wells (Dezayes *et al.*, this issue).

A network of 26 faults could be constructed in a 30x20x6 km model of the sedimentary cover and the top basement representing the faults as surfaces. The orientation of the major and generally synthetic faults (i.e. dipping eastward) is N22.5±7.5°E, whereas a second set strikes N0±10°E (mainly dipping westward), and a third one N45±10°E. The average dip of the faults is 60°. The fault density is approximately 3.7.10<sup>-4</sup> m<sup>2</sup> of faults per cubic meter.

The resulting 3D geological model confirms the tectonic situation of the Soultz site as a horst structure and indicates a maximum vertical offset of

approximately 500m of the basement in the area of the Soultz geothermal anomaly.

A comparison between the smaller scale 3D fractured reservoir model based on borehole imaging, microseismicity and vertical seismic profiling (Sausse *et al.*, 2010) and our 3D regional structural model suggests a strong correlation between the orientation of the partly stimulated fracture zones observed at reservoir scale and the secondary set of faults observed in our regional model.

### **INTRODUCTION**

The geothermal anomaly of the Enhanced Geothermal Systems (EGS) European test site Soultz is strongly related to the existence of zones of relatively high hydraulic conductivity allowing heat transport by fluid circulation. Large hydraulic permeabilities favour the onset of convection and enhances the efficiency of thermal transport in the subsurface. The enhanced surface heat flux in the Upper Rhine valley has been related to the circulation of thermal water along fault zones (Illies 1965). Numerical simulation of the geothermal site of Landau have confirmed this hypothesis (Bachler *et al.*, 2003). The relatively low natural permeability in the 5 km deep reservoir at Soultz is, however, insufficient for economic exploitation. The deep reservoir has been stimulated in a series of hydraulic and chemical stimulations and transmissivity has been enhanced by a factor of up to 10 (Genter *et al.*, 2010). The microseismicity reveals a preferential stimulation of fractures with orientation parallel to

the local stress field, which is in a slight angle to the main faults observed in the regional geological context.

Geological 3D models have been designed across the major geothermal anomalies at Soultz (Renard and Courrioux 1994; Dezayes *et al.*, 2009; Schill *et al.*, 2009), Landau and Speyer (Schill *et al.*, 2009). These earlier geological models of the Soultz area are usually based on five seismic lines (Cautru J.P. (1988) in Menjot *et al.*, 1988), which are located around the reservoir area and the horst structure of Soultz. They present a good overview of the local N-S trending structures.

To enhance the picture of the geological structures and investigate the occurrence of further families of fault parallel to the stimulated fractures on regional scale, we included new datasets to the model of (Dezayes *et al.*, 2009). Firstly, the faults and layers were adapted to the new interpretations of eight recently reprocessed regional seismic lines and former isohypse interpretations (Foehn 1985) down to the Triassic sediments, allowing for a geometrically consistent structural model in the sedimentary cover down to the top of the basement at the regional scale.

### **GEOLOGICAL SETTINGS:**

The Soultz horst structure is located at the western boundary of Upper Rhine Graben (URG), which reveals strong brittle deformation in this section (Fig. 1). While the main orientation of the boundary fault in the area of Soultz is about N52° (Geiermann and Schill 2010), the Mesozoic sediments are affected by a series of subvertical normal faults with a Rhenish (N-S) strike direction in the area of the horst structure.

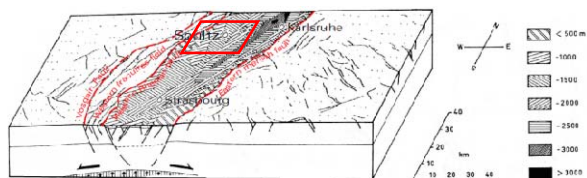


Figure 1: Bloc diagram of the Soultz area. Red rectangle is the showing the model perimeter. Various hatching corresponds to the thickness of the Cenozoic fill. Modified after (Valley 2007).

The Mesozoic platform sediments, which deposited in the Triassic (namely Buntsandstein, Muschelkalk and Keuper) and the Jurassic times (Lias and Dogger) on the peneplaned Variscan basement, rest discordantly on this Permo-Carboniferous series

which was affected by crustal discontinuities (Schumacher 2002).

A general synthesis of the Cenozoic tectonic history of the URG with a special focus on Soultz granite is described in (Valley 2007):

The Soultz granites intruded in Visean time (Early Carboniferous) (Cocherie *et al.*, 2004), during the orogenesis of the Variscan Belt in Europe, resulting from the collision of Laurasia and Gondwana (Franke 1989). During this orogenic stage, they have been affected by a main NE-SW orientation as seen in the neighboring outcrops and several geophysical studies (Edel *et al.*, 2007).

The later Cenozoic rift systems in Europe originates from the Alpine and Pyrenean collisions (Ziegler 1992). The URG can be regarded as typical example of synorogenic intracontinental foreland rifting (Schumacher 2002; Dèzes *et al.*, 2004; Cloetingh *et al.*, 2010). According to (Villemin and Bergerat 1987) and (Villemin *et al.*, 1986) the tertiary tectonic history of the URG occurred on four phases.

The first phase was characterised by a N-S compression and took place in middle to late Eocene. It reactivated Variscan Permo-carboniferous and Mesozoic crustal scale faults in the URG (Dèzes *et al.*, 2004). The second phase was an E-W extension that represents the main rifting stage of graben formation. The extension took place from the end of the Oligocene to that of the Eocene. In early Miocene, a NE-SW oriented compressive phase took place on Rhine Graben shoulders and surrounding and also in Sarre basin. From late Miocene up to the present, the stress regime prevailing in the Rhine Graben is the NW-SE compression that is seen over much of western Europe.

The geothermal reservoir of Soultz is located in a low permeable naturally fractured and hydrothermalized granite primarily related to major faults and fractures zones which, in turn, are connected to dense networks of small-scale structures (Dezayes *et al.*, 2010). The orientation of these fracture zones were estimated using imaging tools such as FMI and UBI revealing a dominant NNW-SSE direction which is different to the Rhenish orientation of large scale fault (Dezayes *et al.*, 2010).

### **NEW DATA COMPILATION:**

Our regional model is based on different recently accessible data among those, recently re-processed and re-interpreted seismic lines, information from oil and geothermal wells and geological maps (Dezayes *et al.*, this issue). These are: 69 boreholes with a mean depth of about 1km and 10 seismic profiles

acquired in the 70's and the 80's for the oil exploration and reprocessed in the framework of different project (Dezayes *et al.*, this issue) (Fig.2). We have also integrated about 15 former seismic profiles and the earlier interpretation of the fault network (Foehn 1985) to compare with our model. This fault network was described in the sedimentary cover based on a dense network of 42 seismic lines acquired in the 70-80's with a mean spacing of 1.5 km.

These data have been homogenized to be entered in a same referential. For that, we have transformed the time scale seismic profile into depth scale cross-section. The seismic horizons were converted from time to depth using velocities of the compressive seismic waves ( $V_p$ ) extracted from 7 regional boreholes (Fig.2) in which the measurements  $time=f(depth)$  were done (Fig.3).

The interval velocity of each formation 'i' can be defined as:

$$\text{Eq. 1: } V_p(i) = \frac{\Delta z(i)}{\Delta t(i)}$$

between the considered depth interval.

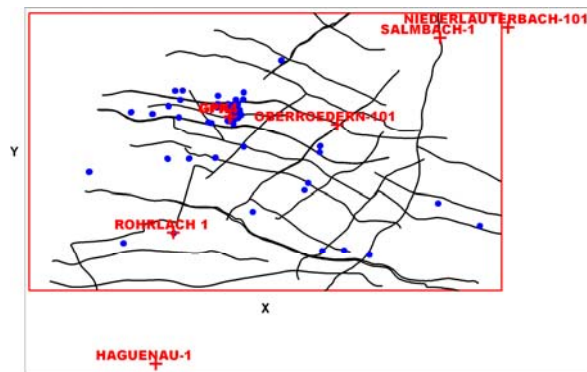


Figure 2: Model perimeter. Where black lines, blue dots and red crosses respectively show seismic lines, boreholes and the 7 boreholes where  $time=f(depth)$  measurements were done.

The information on the thickness of the major formation the area of Soultz obtained from both sources oil and geothermal wells is summarized in Table 1.

Table 1 (top right): Formations thickness observed in the 69 boreholes from oil and geothermal production

Attribute \ Formation	Formation Thickness (m)	Number of boreholes crossing the formation
Tertiary	750 ±320	69
Jurassic	148 ±76	59
Keuper	135 ±58	54
Muschelkalk	130 ±47	20
Buntsandstein	373 ±66	9

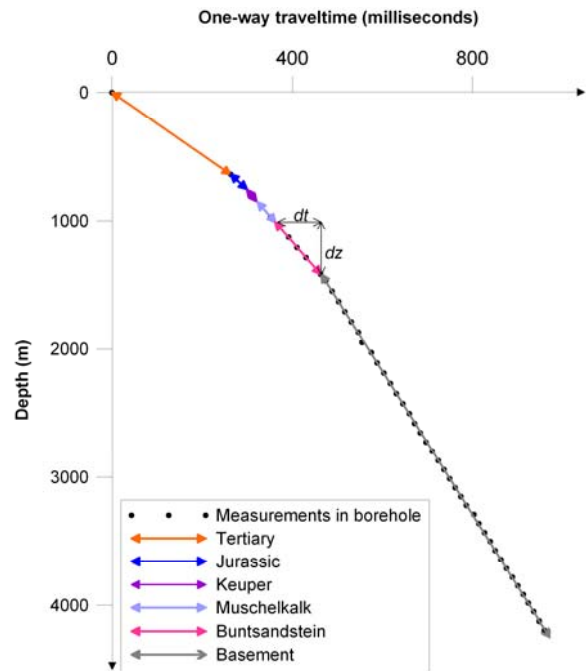


Figure 3: Representative example of the relation between one-way travel time and depth in borehole GPK4.

## METHODOLOGY

### 3D interpretation

Implicit 3D geological modeling provides a powerful tool extrapolate in particular complex fault geometries derived from 2D cross sections such as seismic profiles and borehole data to unknown parts of the model (Renard and Courrioux 1994; Castera *et al.*, 2008).

On the basis of an implicit approach geology can be modeled using the location of the geological interfaces and orientation data from structural field and 2D cross-sections. Both types of data are cokriged to interpolate a continuous 3D potential-

field function describing the geometry of the geology (Calcagno *et al.*, 2008), in which the dip of the layers represents the gradient of the field. 3DGeomodeller (BRGM, Intrepid Geophysics) was used in this study. It offers the possibility to create such geological model and generate various predicted geophysical responses or forward models from it, as well as to compare the 3D geological model against independently gathered geophysical datasets (Guillen *et al.*, 2008).

### **Faults**

The 3D interpretation consists firstly in defining the size of faults and linking them to each seismic profile to build a consistent fault network (Renard and Courrioux 1994; Castera *et al.*, 2008). The integration of the former structural maps, more dense in terms of seismic profiles and the seismic lines largely influenced our choice. We did not include smaller scale faults although they were visible on the seismic lines, because the correlation between the profiles was unclear. The faults have a defined elliptical shape and influence radius on the horizons.

### **Horizons**

The stratigraphic pile was simplified. The modeled horizons are: Tertiary, Jurassic, Keuper, Muschelkalk, Buntsandstein, and the Basement. The Triassic series (Keuper, Muschelkalk, Buntsandstein) are explicitly sub parallel, they rest on the basement series and are covered by the Tertiary series.

### **Statistics**

The calculated 3D structural model including all modeled fault zones is exported as triangulated surfaces, which contain information on strike and dip. These can be plotted in stereoplots and rose diagrams and be analyzed with classical structural approaches. The density of faults is described in  $m^2$  of faults per  $m^3$ .

## **RESULTS**

### **Velocity analysis**

We compare (Tab. 2) the interval velocities extracted from the 7 boreholes time=f(depth) measurements to different type of measurements:

- Standard values for P-wave seismic velocities ( $V_p$ ) in rocks (Kearey and Brooks 1991; Mari *et al.*, 1998)
- Ultrasonic velocities measurements on the core material from borehole EPS1 (Rummel and König 1991)

-Vertical seismic profiles analysis (VSP) (Place *et al.*, 2010)

-Sonic logs corrected by VSP in GPK1 (Beauce *et al.*, 1991)

-Tomographic studies around Soultz reservoir (Horálek *et al.*, 2008).

Even though the thicknesses and the constitutive materials of the different layers is variable in space, the values are in good agreement with  $V_p$  found in the literature (cf. Tab. 2), and are in the same range as measurements on the core material from the geothermal exploration borehole EPS1, as well as the VSP analysis and sonic logs available in well GPK1. An important variability (>15%) in the  $V_p$  of the Jurassic and Muschelkalk serie is noticeable among the different types of measurements.

### **Structural model**

The new regional 3D geological model of the Soultz area covers a volume of 31km X 18.5km X 6km including the sedimentary cover and the top of granitic basement and its structural features.

A number of 26 faults zones crossing the Mesozoic sedimentary layers and the top of the granitic basement could be constructed (Fig. 4).

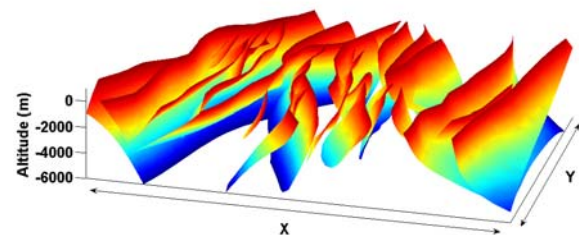


Figure 4: 3D representation of the fault planes

The 3D structural model at the regional scale shows at least three main orientations concerning the faults (Fig.5).

The orientation of the major and generally synthetic faults (i.e. dipping eastward) is  $N22.5 \pm 7.5^\circ E$ , whereas a secondary set strikes  $N0 \pm 10^\circ E$  (mainly dipping westward), and a third one  $N45 \pm 7.5^\circ E$ .

The first set represent about 30 % of the faults, the second one 33% and the third one 25%.

This fault network is only representative for the structural settings in the sedimentary cover since the resolution of faults using seismic remains mainly limited to this part.

Table 2: Comparison between interval velocities for the different formations used in the geological model and the literature

Name of the Serie	Interval velocity in this study: Vp (Km/s)	Standard deviation between boreholes (%)	Constitutive materials	Compressive wave velocities in rocks in literature: Vp (Km/s)	Ultrasonic velocities measurements on the core material from borehole EPS1(Km/s)	VSP measurements and sonic logs corrected by VSP in borehole GPK1 (Km/s)	Tomographic study around the reservoir (Km/s)
Tertiary	2.30±0.07	3.0	Limestone/Marl/Sands tone	2.0-6.0/2.0-3.0/2.0-2.5	ND	ND	≈2.28*
Jurassic	3.57±0.60	16.7	Jurassic Limestone/Marl	3.0-4.0/2.0-3.0	ND	ND	≈3.15*
Keuper	4.11±0.20	4.9	<b>Marl/dolomite</b> /limestone/sandstone	<b>2.0-3.0/2.5-6.5</b> /3.5-6.0/2.0-6.0	ND	ND	≈3.15-3.71*
Muschelkalk	4.63±0.91	19.7	<b>Marl/Dolomite</b> /Sandstone/Limestone	<b>2.0-3.0/2.5-6.5</b> /2.0-6.0/3.5-6.0	5.35 ± 0.28	3.62±0.1	3.71
Buntsandstein	4.44±0.58	13.0	Sandstone/Conglomerate	2.0-6.0/not available	4.53±0.51	4.33±0.03	4.54
Basement	5.61±0.04	0.8	Porphyric monzogranite/ Fine-grained two-mica granite	5.5-6.0	5.51±0.02	5.64 5.66 5.78	5.48 5.89

\*depth intervals chosen in the tomographic study were not chosen the same as the ones encountered in the geothermal wells, this can lead to differing values

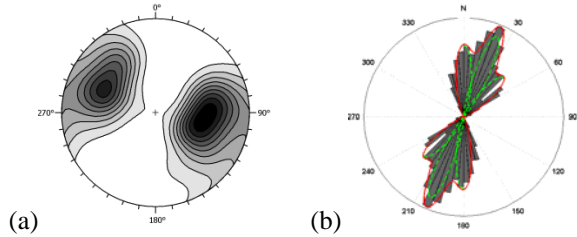


Figure 5: a) Stereographic projection of triangulated fault surfaces poles density for each triangle of the 3D model (lower hemisphere, equal area). The isolines represent 10% population intervals - b) Circular histogram of faults strike (in grey). Each set is highlighted by two symmetric green petals (Gaussian repartition). The red contour is the sum of the green petals.

The fault density is approximately  $3.7 \cdot 10^{-4} \text{ m}^2$  of faults per cubic meter.

Minor faults (not included in the model but present on the seismic profiles) are measured to be about 0.9 fault per km in the E-W direction and about 0.5 fault per km in the N-S direction and seem to follow the same trend as the one included in our model.

The resulting 3D geological model confirms the tectonic situation of the Soultz site as a horst structure and indicates a maximum vertical offset of approximately 500 meters of the basement under Soultz site (Fig. 6), in the area of the geothermal anomaly (Fig. 7).

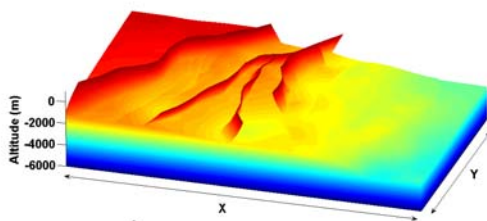


Figure 6: 3D model showing the depth of the top basement, the horst structure with its three main faults and the graben western border fault.

## DISCUSSION

The orientation of the different fault sets can be related to the tectonic history of the Upper Rhine Graben.

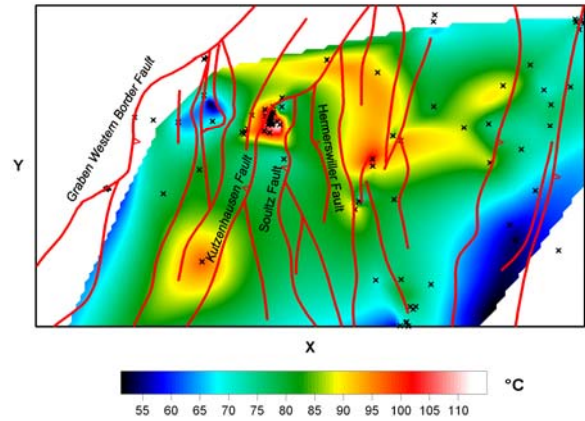


Figure 7: Superposition of the surface faults (in red) and the temperature field at 800m depth (data provided by LIAG-Hannover).

Most of the sets are probably due to the first and second main rifting phase of the Upper Rhine Graben, characterized by a N-S compression and an E-W extension which took place from the end of the Oligocene to that of the Eocene respectively (Villemain 1986) A geodynamical approach based on the present 3D model statistics could infer these interpretations.

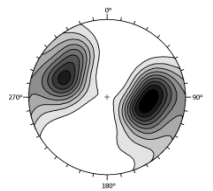
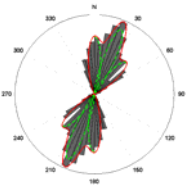
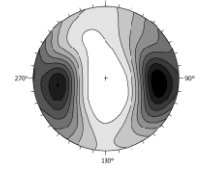
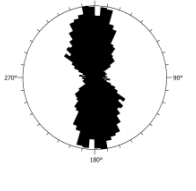
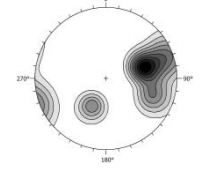
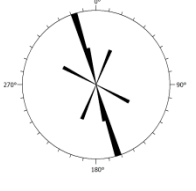
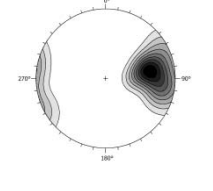
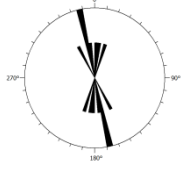
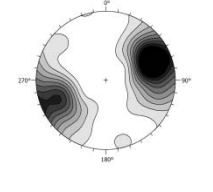
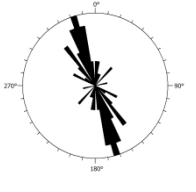
To get insights on the possible connection of these faults to the basement we compare the 3D reservoir model of Soultz based on borehole imaging, VSP and microseismicity during stimulation, designed in (Sausse *et al.*, 2010).

As shown in Table 3, the secondary and antithetic fault network observed in our analysis (Fig. 6) with a mean direction of  $N0 \pm 10^\circ E$  dipping at  $60 \pm 8^\circ$  dominantly to the west and the major fracture zone network in the granite reveal similar strike direction and dip direction:

- VSP: mean strike  $N165^\circ E$ , dipping at  $75^\circ$  dominantly to the west
- Microseismicity:  $N165^\circ E$ ,  $70^\circ$  to the west
- Fracture zones:  $N165^\circ E$ ,  $65^\circ$  to the west

The comparison of the fractures orientations observed in the Buntsandstein layer and the granitic basement however suggests a continuity in the deformation between the two formations (Dezayes *et al.*, 2010). The occurrence of a same family of directions of faults in the sedimentary cover and the fractures in the basement suggests similar results.

This secondary set of faults is likely to be stimulated during fracturation its orientation being parallel to the local stress field.

Data	Poles	Faults Strike
(A) 3d Model: Triangulated Surfaces		
(B) Boreholes Fractures: 4141 Data		
(C) VSP: 5 Data		
(D) Microseismicity: 7 Data		
(E) Fractures Zones: 41 Data		

In addition, the average spacing of about 500 meters between the major fracture zones highlighted in (Dezayes *et al.*, 2010) is consistent with the fault spacing in our model.

## CONCLUSIONS

The construction of the 3D structural model of Soultz region satisfies information from different sources.

The resulting fault network in the sedimentary cover was analyzed in terms of orientation, related to the tectonic history of the URG and compared with the deep granite fractures network.

Table 3 (left): a) Poles density and circular histograms of faults in the 3D model (lower hemisphere, equal area), The isolines represent 10% population intervals – b) Poles density of all fractures observed in boreholes GPK3 and GPK4 below the depth of 1450m (granitic basement) - c) Poles density of fractures observed by VSP (Sausse *et al.*, 2010) - d) Poles density of fractures observed by microseismicity (Sausse *et al.*, 2010) – e) Poles density of natural flowing fracture zones based on borehole imaging and other borehole geophysical measurements (Sausse *et al.*, 2010).

It appears that one set of secondary faults in the present model has similar strike and dip direction to the ones of the fractures observed in the deep granite reservoir of Soultz based on borehole imaging, VSP and microseismicity during stimulation, designed in (Sausse *et al.*, 2010). This suggests a continuity in the deformation between the two formations.

This secondary set of faults is likely to be stimulated during fracturation its orientation being parallel to the local stress field.

## ACKNOWLEDGEMENTS

The authors would like to thank BRGM, GEIE Soultz and LIAG-Hannover for providing data, Pierrick Altwegg, Andrea Borghi, Philippe Renard, Benoit Valley for their technical assistance, and Yassine Abdelfettah for his constant availability and his assistance in the geophysical processing.

## REFERENCES

- Bachler, D., T. Kohl and L. Rybach (2003). "Impact of graben-parallel faults on hydrothermal convection - Rhine Graben case study." *Physics and Chemistry of the Earth* **28**(9-11): 431-441.
- Beauce, A., H. Fabriol, D. Le Masne, C. Cavoit, P. Mechler and X. Kai Chen (1991). "Seismic studies on the HDR site of Soultz-Sous-Forêts (Alsace, France)." *Geotherm. Sci & Tech.* **3**(1-4): pp. 239-266.
- Calcagno, P., J. P. Chiles, G. Courrioux and A. Guillen (2008). "Geological modelling from field data and geological knowledge Part I. Modelling method coupling 3D potential-field interpolation and geological rules." *Physics of the Earth and Planetary Interiors* **171**(1-4): 147-157.

- Castera, J., C. Dezayes and P. Calcagno (2008). "Large-scale 3D geological model around the Soultz site." Proceedings of the EHDRA scientific conference 24-25 September 2008, Soultz-sous-forêts, France.
- Cautru J.P. (1988) in Menjot, A., J. P. Cautru, A. Criaud and A. Genter (1988). "Roches sèches chaudes. Caractérisation des réservoirs fracturés." Rapport annuel d'activités 1988n BRGM/IRG: 35-39.
- Cloetingh, S., J. D. van Wees, P. A. Ziegler, L. Lenkey, F. Beekman, M. Tesauro, A. Förster, B. Norden, M. Kaban, N. Hardebol, D. Bonté, A. Genter, L. Guillou-Frottier, M. Ter Voorde, D. Sokoutis, E. Willingshofer, T. Cornu and G. Worum (2010). "Lithosphere tectonics and thermo-mechanical properties: An integrated modelling approach for Enhanced Geothermal Systems exploration in Europe." Earth-Science Reviews **102**(3-4): 159-206.
- Cocherie, A., C. Guerrot, C. M. Fanning and A. Genter (2004). "Datation U-Pb des deux faciès du granite de Soultz (Fossé rhénan, France)." Géochimie (Géochronologie) **336**(9): 775--787.
- Dezayes, C., L. Becalotto, G. Oliviero, P. Baillieux, L. Capar and E. Schill (2011). "3-D visualization of a fractured geothermal field: the example of the EGS Soultz site (Northern Upper Rhine Graben, France)." PROCEEDINGS, Thirty-Sixth Workshop on Geothermal Reservoir Engineering Stanford University (this issue).
- Dezayes, C., J. Castera, G. Heilbronn and P. Calcagno (2009). "Regional geological model of the Soultz-sous-Forêts geothermal field (Rhine Graben, France). ." GRC transactions, Vol. 33: 175-180.
- Dezayes, C., A. Genter and B. Valley (2010). "Overview of the Fracture Network at Different Scales Within the Granite Reservoir of the EGS Soultz Site (Alsace, France)." Proceedings World Geothermal Congress 2010 Bali, Indonesia, 25-29 April 2010.
- Dezayes, C., A. Genter and B. Valley (2010). "Structure of the low permeable naturally fractured geothermal reservoir at Soultz." C. R. Geoscience **342**(2010): 517-530.
- Dèzes, P., S. M. Schmid and P. A. Ziegler (2004). "Evolution of the European Cenozoic Rift System: interaction of the Alpine and Pyrenean orogens with their foreland lithosphere." Tectonophysics **389**: 1--33.
- Edel, J. B., K. Schulmann and Y. Rotstein (2007). "The Variscan tectonic inheritance of the Upper Rhine Graben: evidence of reactivations in the Lias, Late Eocene-Oligocene up to the recent." International Journal of Earth Sciences.
- Foehn, J. P. (1985). "interprétation des campagnes sismiques 1981 et 1984, concession de Pechelbronn, permis de Haguenau. Total Exploration internal report, October 19985."
- Franke, W. (1989). "Variscan plate tectonics in Central Europe--current ideas and open questions." Tectonophysics **169**(4): 221-228.
- Geiermann, J. and E. Schill (2010). "2-D Magnetotellurics at the geothermal site at Soultz-sous-Forêts: Resistivity distribution to about 3000 m depth." Comptes Rendus Geoscience **342**(7-8): 587-599.
- Genter, A., K. Evans, N. Cuenot, D. Fritsch and B. Sanjuan (2010). "Contribution of the exploration of deep crystalline fractured reservoir of Soultz to the knowledge of enhanced geothermal systems (EGS)." Comptes Rendus Geoscience **342**(7-8): 502-516.
- Guillen, A., P. Calcagno, G. Courrioux, A. Joly and P. Ledru (2008). "Geological modelling from field data and geological knowledge Part II. Modelling validation using gravity and magnetic data inversion." Physics of the Earth and Planetary Interiors **171**(1-4): 158-169.
- Horálek, J., Z. Jechumtálová, L. Dorbath and J. Šílený (2008). "Shear vs. non-shear components in source mechanisms of microearthquakes induced in hydraulic fracturing experiment at the HDR site Soultz-Sous-Forêts (Alsace) in 2003." EHDRA scientific.
- Illies, J. H. (1965). "Bauplan und Baugeschichte des Oberrheingrabens. Ein Beitrag zum "Upper Mantle Project". " Oberrheinische Geologische Abhandlungen **14**: 1-54.
- Kearey, P. and M. Brooks (1991). "An introduction to Geophysical Exploration." 2nd ed. ix + 254 pp. Oxford: Blackwell Scientific Publications.
- Mari, J.-L., G. Arens, D. Chapellier and P. Gaudiani (1998). "Géophysique de Gisement et de Génie Civil." Institut Français du Pétrole.
- Place, J., M. Diraison, C. Naville, Y. Géraud, M. Schaming and C. Dezayes (2010). "Decoupling of deformation in the Upper Rhine Graben sediments. Seismic reflection and diffraction on 3-component Vertical Seismic Profiling (Soultz-sous-Forêts area)." C. R. Geoscience **342**(2010): 575--586.
- Renard, P. and G. Courrioux (1994). "Three-dimensional geometric modeling of a faulted



- domain: The Soultz Horst example (Alsace, France)." Computers & Geosciences **20**(9): 1379-1390.
- Rummel, F. and E. König (1991). Physical properties of Core samples, borehole EPS1, Soultz-sous-Forêts: Velocity-, Density- and magnetic susceptibility- logs, depth interval 933-2227 m. Yellow report 6. Bochum, Ruhr - Universität: 58.
- Sausse, J., C. Dezayes, L. Dorbath, A. Genter and J. Place (2010). "3D fracture zone network at Soultz based on geological data, Image logs, microseismic events and VSP results." C.R. Geoscience **342** (2010): 531-545.
- Schill, E., T. Kohl, C. Baujard and J.-F. Wellmann (2009). "Geothermische Ressourcen in Rheinland-Pfalz: Bereiche Süd- und Vorderpfalz, Final report to the Ministry of Environment Rhineland-Palatine, 55p."
- Schumacher, M., E. (2002). "Upper Rhine Graben: Role of preexisting structures during rift evolution." Tectonics **21**(1): 1006.
- Valley, B. (2007). "The relation between natural fracturing and stress heterogeneities in deep-seated crystalline rocks at Soultz-sous-Forêts (France), PhD thesis, ETH-Zürich, Switzerland, <http://e-collection.ethbib.ethz.ch/view/eth:30407>, 260 p."
- Villemin, T. (1986). Tectonique en extension, fracturation et subsidence : Le Fossé Rhénan et le bassin de Sarre-Nahe. Paris VI. Paris, Paris VI. **PhD**: 270.
- Villemin, T., F. Alvarez and J. Angelier (1986). "The Rhinegraben: Extension, subsidence and shoulder uplift." Tectonophysics **128**(1-2): 47-59.
- Villemin, T. and F. Bergerat (1987). "L'évolution structurale du fossé rhénan au cours du Cénozoïque : un bilan de la déformation et des effets thermiques de l'extension." Bulletin de la Société Géologique de France **3**(2): 245--255.
- Ziegler, P. A. (1992). "European Cenozoic rift system." Tectonophysics **208**(1-3): 91-111.